RAPID COMMUNICATION

High-power narrow-linewidth diode laser based on external cavity feedback technology for Yb: YAG pumping

https://doi.org/10.35848/1347-4065/aca247

High-power narrow-linewidth diode laser based on external cavity feedback technology for Yb: YAG pumping

Jinliang Han[1,2], Jun Zhang[1*], Xiaonan Shan[1], Yawei Zhang[1], Hangyu Peng[1], Li Qin[1], and Lijun Wang[1]

[1]Changchun Institute of Optics, Fine Mechanics and Physics, Chinese Academy of Sciences, Changchun 130033, People's Republic of China
[2]University of Chinese Academy of Sciences, Beijing 100049, People's Republic of China

*E-mail: zhangjciomp@163.com

Received October 3, 2022; revised October 23, 2022; accepted November 11, 2022; published online November 24, 2022

An external cavity feedback structure based on volume Bragg grating is introduced to realize the spectral stabilization and linewidth narrowing of a diode laser with a central wavelength of 968.668 nm and a spectral linewidth of 0.405 nm. A diode laser source producing 1.443 kW power from an output fiber with a core diameter of 1000 μm is achieved by using a spatial beam, combining, and polarization multiplexing technologies. The external cavity feedback and fiber coupling efficiencies exceed 93% and 90%, respectively. Such a high-power narrow-linewidth diode laser can be applied in Yb: YAG pumping efficiently and stably.

With the development of high-efficiency laser diode (LD) and LD array technology, diode-pumped solid-state lasers (DPSSLs) have been developed rapidly.[1–3] DPSSLs have many advantages, such as high-efficiency, high-power output, compactness, long operation lifetime, and excellent beam quality, which demonstrates their superiority to lamp-pumped solid-state lasers.[4,5] In 1965, L. F. Johnson from Bell Laboratories realized Yb: YAG laser operation for the first time by using flash lamp pumping at a temperature of 77 K.[6] However, the optical-to-optical conversion was inefficient due to the inefficient matching between the Yb^{3+} absorption spectrum and the pumping spectrum of the flash lamp. Therefore, Yb: YAG crystals were ignored at that time. In the early 1990s, InGaAs LD appeared and developed rapidly, which makes high-power diode laser a stable pumping source, and Yb^{3+}-doped crystal material attracted the attention of researchers due to its excellent laser properties, such as simple energy level structure, high quantum efficiency, and long fluorescence lifetime.[7–9] At present, diode laser-pumped Yb: YAG laser can achieve kilowatt class output power, which has an important value in laser cutting, welding, milling, and medical applications.[10–14]

Figure 1 shows the absorption and emission spectra of Yb: YAG crystal.[15] Yb: YAG crystal has two absorption bands, which are located around 940 and 969 nm, respectively. The absorption linewidth of 940 nm is relatively wide, so the requirements for the linewidth and central wavelength of the pumping source are not strict. However, the absorption linewidth of 969 nm is narrow, so the central wavelength should be controlled within 969 nm ± 0.5 nm, and the spectral linewidth should be controlled less than 1 nm. The diode laser as the pumping source has the typical spectral linewidth of 2 nm to 5 nm, which is wide to pump Yb: YAG at 969 nm. The drift of the central wavelength with temperature is remarkable, so the pump and absorption spectra cannot be strictly matched. Thus, the spectral linewidth must be narrowed, and the central wavelength should be locked strictly by technical means. At present, the main method is to use a diode laser at 940 nm to pump Yb: YAG gain medium. Shinki Nakamura et al. reported a diode-end-pumped high-efficiency high-power Yb: YAG ceramic laser. A 940 nm fiber-coupled diode laser was used as a pumping source, the core diameter of the fiber was 200 μm, and the numerical aperture (NA) was 0.22. When the pumping power of the diode laser was 13.8 W, a 6.8 W CW output power was obtained with a slope efficiency of 72%.[16] Gangfei Ma et al. reported a compact CW yellow laser source at 578 nm by using doubly resonant with a folded overlapped cavity and intracavity sum-frequency mixing of thin-disk Yb: YAG laser and Nd: YAG laser with lithium triborate crystal. A diode laser emitting at the wavelength of 940 nm with an output power of 13.2 W was used to pump Yb: YAG disk crystal for 1030 nm oscillation.[17] Fengjiang Zhuang et al. used a fiber-coupled diode laser with a wavelength of 940 nm for the longitudinal pumping of the Yb: YAG laser rod. The output of the laser diode was not polarized, delivering a maximum optical pump power of about 21 W at 940 nm after going through a pair of coupling lenses. The average output power reached 3.55 W at the maximum pump power of 21 W at 15 °C of a thermoelectric cooler.[18]

Pumping Yb: YAG gain medium at 969 nm has obvious technical advantages. The emission wavelength is 1030 nm when Yb: YAG gain medium is stimulated. In the process of pumping Yb: YAG, a quantum defect occurs, and the lost energy produces heat directly, which affects the stable operation of the laser. On the basis of the laser principle, the quantum defect q can be expressed as Eq. (1), where λ_1 represents the absorption wavelength, and λ_2 represents the emission wavelength. The quantum defect is about 8.7% when pumping at 940 nm, whereas it is only 5.9% when pumping at 969 nm. No upper energy state absorption and upper energy level conversion occur because of the level of Yb^{3+} with a simple structure, and quantum defect is mostly the reason for heat production. Therefore, pumping Yb: YAG through a diode laser at 969 nm with a narrow-linewidth and stable spectrum has obvious advantages in the generation of 10 kw class or higher power-level lasers, which is a new direction worthy of further research.

$$q = 1 - \frac{\lambda_1}{\lambda_2}. \quad (1)$$

In this study, a diode laser pumping source at the locked wavelength of 968.668 nm with a narrow-linewidth of 0.405 nm is investigated and designed by using the external cavity feedback technology of volume Bragg grating (VBG).[19,20] A diode laser source producing 1.443 kW power from a fiber with a core diameter of 1000 μm and NA of 0.22 is realized. A related previous work has been performed this year. We reported a high-power narrow-linewidth 780 nm diode laser

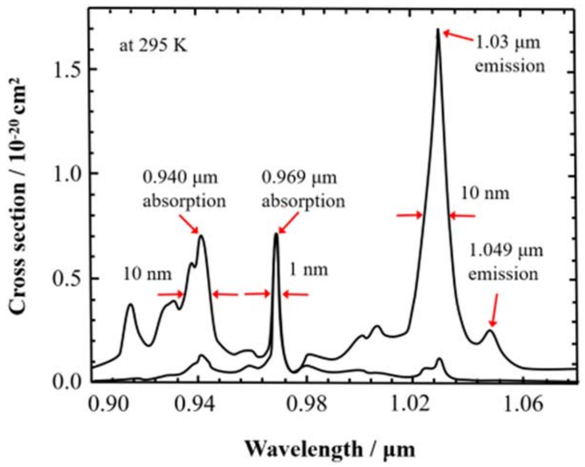

Fig. 1. (Color online) Absorption and calculated emission cross section for Yb: YAG.

based on the external cavity feedback technology of VBG.[21] However, the object in the previous study is a diode laser bar, and the one VBG is used to feedback 19 emitters. The object of the present study is a single emitter, and the one VBG is used to feedback one single emitter. This setting achieves a better external cavity feedback effect than the previous work. The results show a high-power narrow-linewidth diode laser with higher external cavity feedback and fiber coupling efficiencies by combining polarization multiplexing and fiber coupling technologies. These techniques have not been used in previous work. This work demonstrates a reasonable means for Yb: YAG pumping.

In this study, a single emitter diode laser is used as a unit device, and its typical parameters are shown in Table I. High-power laser output can be obtained by beam shaping and beam combination technology. The external cavity feedback technology based on VBG is used to select the mode of the multimode diode laser, and then the spectra narrowing and wavelength locking can be realized. Compared with the linear array and stack structure, the single emitter diode laser structure has no influence on thermal crosstalk. Therefore, the operation reliability can be guaranteed, and the quality of cooling water is not required. The linear array and stack structure have multiple single emitters in a single bar. Hence, the "smile" effect occurs, which has a great influence on the external cavity feedback for spectral locking.[22] The single emitter diode laser can obtain a better spectral locking effect by single VBG, which can avoid this problem effectively.

Table I. Typical parameters of single emitter laser.

Parameters	Unit	Specifications
Central wavelength	nm	969
Central wavelength tolerance	nm	±3
Spectral width (FWHM)	nm	<3
Output power	W	12
Operating current	A	⩽12
Operating voltage	V	<1.9
Emitter width	μm	200
Vertical far field 95% PIB	deg	⩽60
Lateral far field 95% PIB	deg	⩽12
Polarization	/	TE

Figure 2 presents the schematic of beam shaping and spectrum control. The pumping laser system consists of single emitter diode lasers packaged in a chip on a submount structure, fast axis collimations (FACs) and slow axis collimations (SACs) as the beam collimation element, VBGs as a wavelength-selective element, mirrors for spatial beam combining, a half-wave plate and a polarized beam splitter (PBS) for beam polarization multiplexing, and an antireflection mirror (900–980 nm antireflection coating and 1020–1100 nm reflection coating) to protect the 1030 nm emission laser back into the laser cavity.

The divergence angle in the fast axis is usually 30°–60°, and the slow axis is 8°–12°. Therefore, the use of FAC and SAC is necessary to reduce the laser divergence angle for facilitating the subsequent spatial beam combining and beam polarization multiplexing. The FAC adopts an aspheric column lens with a focal length of 0.3 mm. The divergence angle in the slow axis is relatively small, and the SAC adopts a spherical cylindrical lens with a focal length of 20 mm. A simulation is conducted on Zemax software, and the simulation results are shown in Fig. 3. The simulated divergence angle of the single emitter laser after beam shaping is 4 mrad (FWHM) in the fast axis and 10 mrad (FWHM) in the slow axis, respectively. The corresponding spot sizes are 0.36 mm (Y-coordinate value) and 4 mm (X-coordinate value).

Several single emitter lasers are combined by using spatial beam combining and beam polarization multiplexing to scale laser power.[23,24] Ten single emitter lasers are used as a group, and the beams are stacked in the fast axis direction with a step spacing of 0.4 mm. The beam sizes in the fast and slow axes are 4 mm after spatial beam combining, as shown in Fig. 4. The combination of half-wave plate and PBS is adopted to integrate the laser beam of another 10 single emitter lasers through beam polarization multiplexing technology. The power density is doubled while maintaining the beam quality. The output power of the unit module is theoretically greater than 240 W.

Figure 5 shows the structure diagram of the external cavity feedback of the single emitter diode laser. The approximate formula of spectral locking by VBG can be obtained by using the rate equation to understand the mode competition process between the VBG diffraction efficiency and the facet reflectivity of the laser chip front facet,[25] which can be expressed as

$$r_3 \geqslant r_2 \exp\{2\Gamma[g(\lambda_0) - g(\lambda_g)]\mathrm{L}\}, \tag{2}$$

where r_1 is the reflectivity of the rear cavity surface of the diode laser chip, r_2 is the facet reflectivity of the laser chip front facet, r_3 is the diffraction efficiency of VBG, and Γ is the confinement factor of the diode gain region. $g(\lambda)$ is the gain as a function of wavelength, λ_0 and λg are the free-running and VBG locking wavelengths, and the resonant cavity length in the active region and the outer cavity length are represented by l and L, respectively.

However, catastrophic optical mirror damage (COMD) can easily occur in the external cavity feedback structure when the laser output power is high. The low reflectivity of the front facet of the laser chip r_2 likely leads to an increase in the laser power density at the local position of the front facet and then accelerates the damage to the front facet. The diffraction efficiency r_3 of VBG must be increased to satisfy the

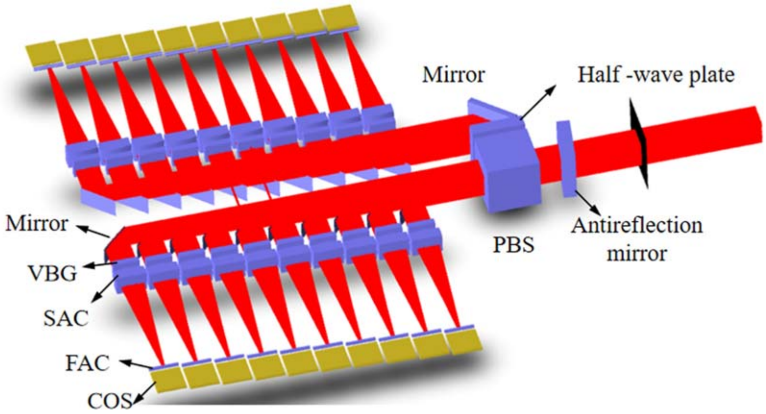

Fig. 2. (Color online) Schematic of beam shaping and spectrum control.

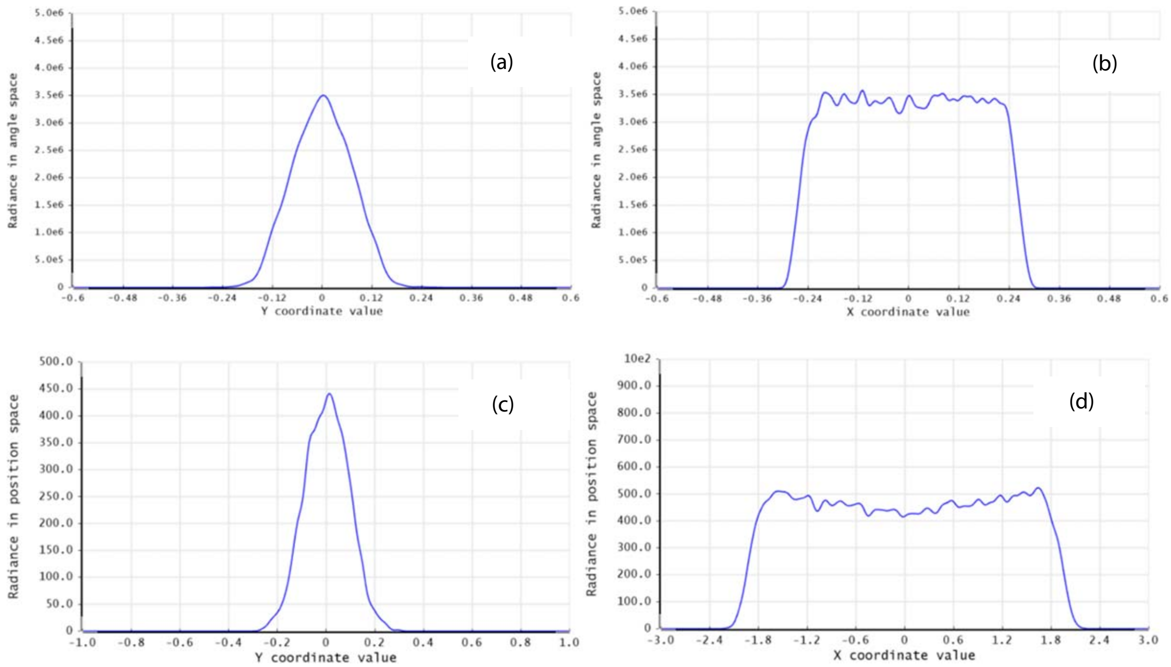

Fig. 3. (Color online) Divergence angle of single emitter laser in the (a) fast axis and (b) slow axis after collimation. Beam size of single emitter laser in the (c) fast axis and (d) slow axis after collimation.

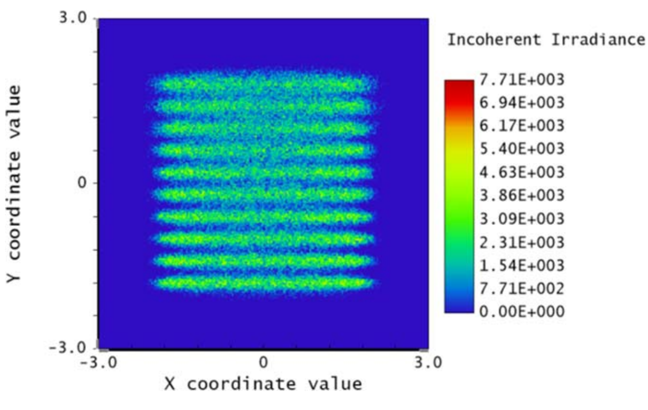

Fig. 4. (Color online) Simulation diagram of laser beam combination.

equation relation when using the laser chip with high reflectivity of r_2. However, increasing the diffraction efficiency of VBG may cause peaks of laser power on the cavity surface and result in COMD.[26] To sum up, the reflectivity of the front facet and the diffraction efficiency of VBG should be selected properly to obtain fine reliability and spectral locking effect. In this study, the reflectivity of the front facet of the laser chip r_2 is set to 2%–3%. The size of VBG with a central wavelength of 968.7 nm ± 0.2 nm is 4.6 mm × 3 mm × 1 mm, and the diffraction efficiency is set to 10%±3%.

A laser module composed of 20 single emitter diode lasers with narrow-linewidth and stable wavelength is developed. Eight laser modules are used to obtain the laser output with high-power of kilowatt class and narrowing linewidth by using spatial beam combining and high-efficiency fiber coupling technologies. The principle of the optical path diagram is shown in Fig. 6. Two layers with four laser modules are used in each layer. The laser modules in each layer are spatially combined into small square spots through a small laser mirror. The laser spots of the lower layer are reflected to the upper layer through a large laser mirror. The combined laser beam of two layers is coupled into a fiber with a core diameter of 1000 μm and NA of 0.22 through an aspheric focusing lens with a diameter of 35 mm and a focal length of 75 mm. The corresponding beam quality is about 110 mm·mrad. The output power of a laser module under free-running and wavelength locking as a function of

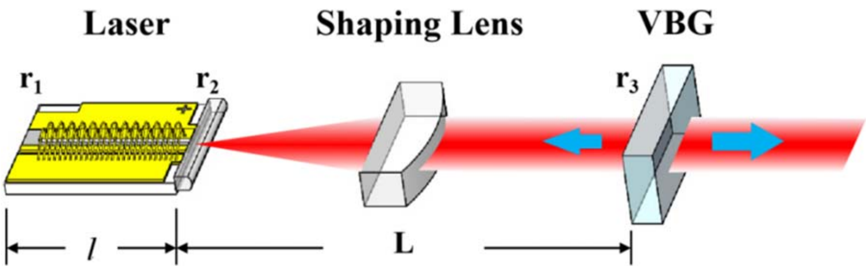

Fig. 5. (Color online) Schematic of external cavity diode laser.

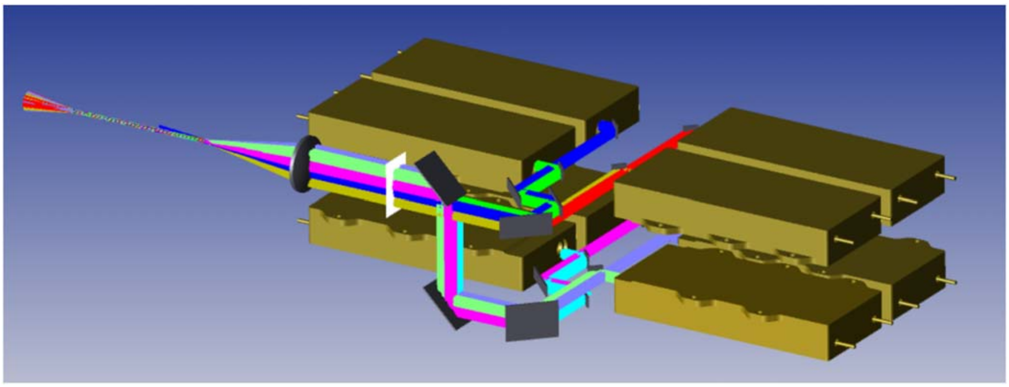

Fig. 6. (Color online) Optical path diagram of high-power narrow-linewidth diode laser.

operating current is shown in Fig. 7. When the water cooling temperature is 22 °C and the operating current is 12 A, the total output power of the 20 single emitters measured by an Ophir power meter is 245.4 W. The test power is 219.2 W with an optical-optical efficiency of 89.32% after the beam collimation, spatial beam combining, and polarization multiplexing. The external cavity feedback efficiency is defined as the ratio of VBG external cavity locking power to free-running power. The locking output power is 205.7 W with an external cavity feedback efficiency of 93.84% after the wavelength locking by VBGs. The output power is lower than the theoretical calculation power due to four conditions: (1) In the spatial beam combining process, the edge laser beam is blocked more or less by optical mirrors in the actual installation and adjustment process. (2) The lenses in the optical path are coated with antireflective film, and the transmissivity is approximately 99%–99.8%. The optical mirrors are coated with reflective film, and the reflectivity is 99%–99.8%. Therefore, a certain power loss occurs during laser transmission. (3) The linear polarization degree of the high-power diode laser chip itself cannot reach 100% transverse electric (TE) polarization or transverse magnetic™ polarization, but is usually 92%–98%. (4) In the process of polarization multiplexing based on PBS, the laser with TE polarization or TM polarization occurs at an angle of 45°. Compared with the ideal condition at the Brewster angle, a certain angle error causes the transmissivity loss of the lens. When the above losses are accumulated, the actual output power is lower than the ideal situation.

The kilowatt class high-power and narrow-linewidth diode laser pumping source is developed on the basis of the above eight laser modules. The physical image of the laser is shown in Fig. 8. When the water cooling temperature is 22 °C and the operating current is 12 A, the total output power of eight laser modules is 1.66 kW. The test power is 1.594 kW with

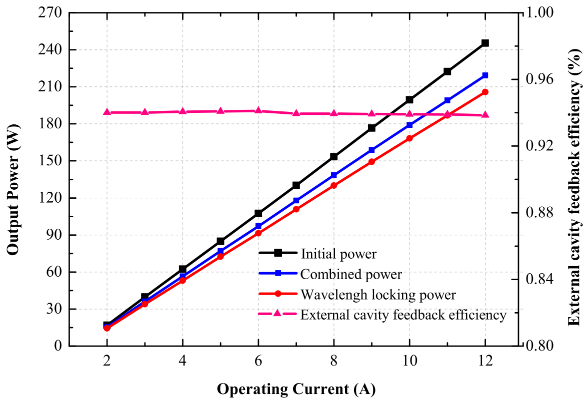

Fig. 7. (Color online) Output power and external cavity feedback efficiency as a function of operating current.

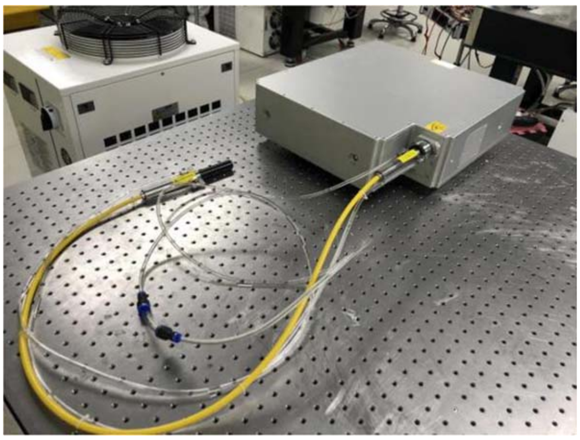

Fig. 8. (Color online) Photograph of high-power narrow-linewidth diode laser.

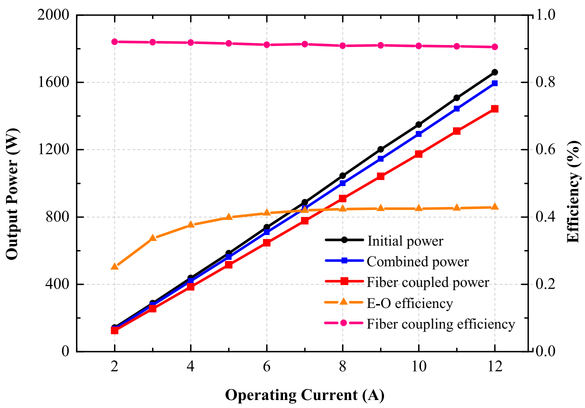

Fig. 9. (Color online) Output power and fiber coupling efficiency as a function of operating current.

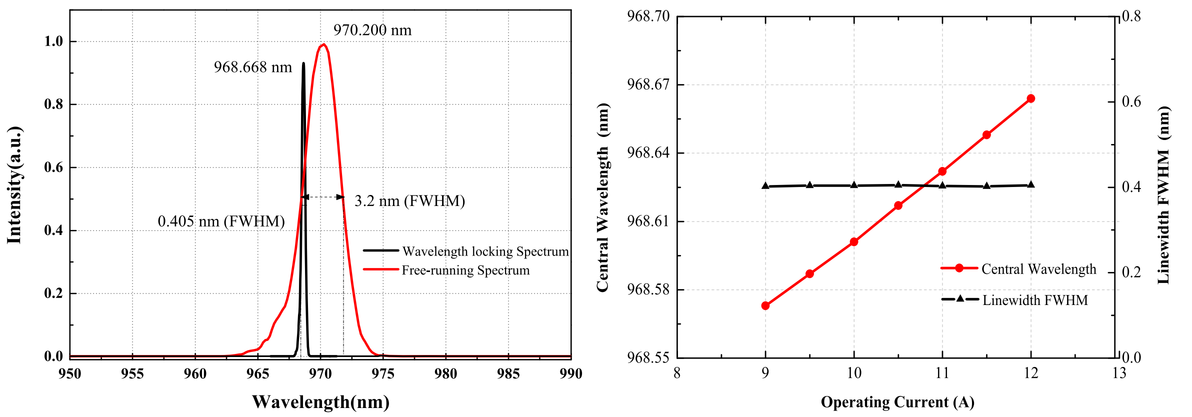

Fig. 10. (Color online) (a) Spectrum of free-running and VBG locking diode laser under 12 A of operating current (b) central wavelength and linewidth after VBG locking as a function operating current.

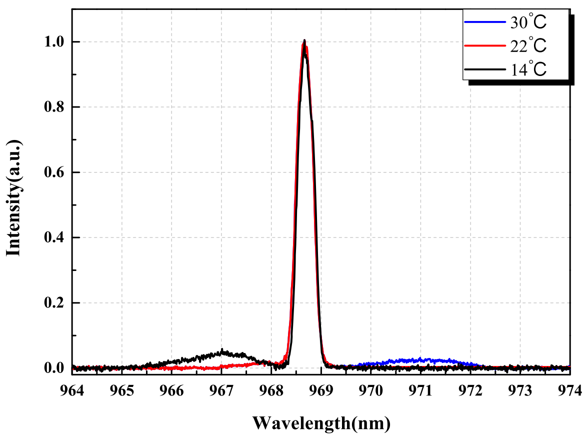

Fig. 11. (Color online) Spectrum of VBG locking diode laser under different working temperature.

3.98% power loss after beam combination. The combined beam is coupled into the fiber through the focusing lens. The experimental results show that the power from the fiber is 1.443 kW with a fiber coupling efficiency of 90.53% and electro-optical efficiency of 42.9%, as shown in Fig. 9.

An Ando AQ6317B fiber spectrometer is used for spectral measurement. The central wavelength and spectral linewidth of the free-running diode laser and the wavelength locking diode laser are compared under the operating current of 12 A, as shown in Fig. 10(a). The central wavelength and spectral linewidth of the free-running diode laser are 970.2 and 3.2 nm, respectively, which cannot meet the pumping requirements of Yb: YAG. The central wavelength and spectral linewidth after wavelength locking by VBG are 968.668 and 0.405 nm, which can meet the high-efficiency pumping requirements of Yb: YAG. The central wavelength and spectral linewidth after wavelength locking as a function of operating current are shown in Fig. 10(b). The spectral linewidth does not change remarkably with the increase in operating current, whereas the central wavelength increases linearly under the same operating conditions, which is consistent with the temperature drift characteristics of VBG. The laser output power increases with the increase in current, so the VBG after laser irradiation produces more heat. The experimental results show that the locked central wavelength shift as a function of the operating current is approximately at the rate of 0.03 nm A^{-1}.

The wavelength locking effect is also closely related to the working temperature. When the working temperature of cooling water is 14 °C, 22 °C, and 30 °C, and the operating current is 12 A, the central wavelengths are 968.666, 968.668, and 968.669 nm, respectively. Changing the working temperature of the cooling water has minimal effect on the central wavelength of the external cavity feedback diode laser. However, the working temperature affects the wavelength of the free-running laser and causes the self-excitation effect of the emitting laser after external cavity feedback, which can influence the pumping efficiency of Yb: YAG, as shown in Fig. 11.

The high-power diode laser should have stable output and spectral characteristics for the efficient pumping of Yb: YAG. The output power and spectral characteristics cannot have a large shift, especially when working for a long time. The output power and spectral characteristics are measured for 2 h of operation time at an operating current of 12 A. The results are shown in Figs. 12(a) and 12(b). The experimental results show that the laser has good output power stabilization and spectral stabilization, which can meet the high-efficiency pumping requirements of Yb: YAG for a long operation time.

An external cavity feedback structure based on VBG is employed to obtain a high-power narrow-linewidth diode laser with a central wavelength of 968.668 nm and a spectral linewidth of 0.405 nm. A CW power of 1.443 kW from an optical fiber with 1000 μm core diameter and 0.22 NA is

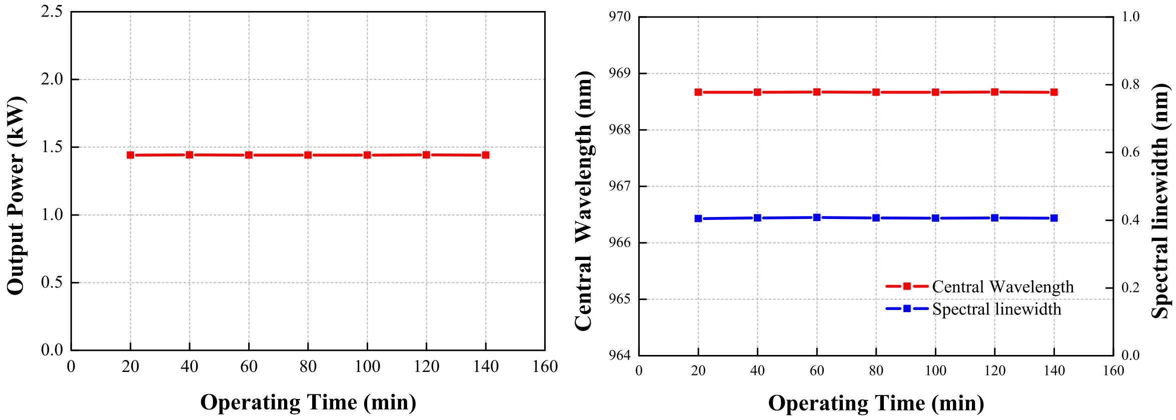

Fig. 12. (Color online) Variation of (a) output power (b) central wavelength and spectral linewidth with operation time.

realized by using spatial beam combining and polarization multiplexing technologies. The external cavity feedback and fiber coupling efficiencies exceed 93% and 90%, respectively. This laser source with a quantum defect of 5.9% can be used to pump Yb: YAG efficiently and stably. In this study, the central wavelength of the output laser cannot be tuned. Further research is needed to tune the central wavelength by controlling the temperature of VBG.

Acknowledgments This work was supported by the Natural National Science Foundation of China (NSFC) (61991433, 62121005), Pilot Project of CAS (XDB43030302), Equipment Pre Research (2006ZYGG0304, 2020-JCJQ-ZD-245-11), Key Research and Development Project of Guangdong Province (2020B090922003).

1) H. An, C. Jiang, Y. Xiong, A. Inyang, Q. Zhang, A. Lewin, S. Strohmaier, and G. Treusch, Proc. of SPIE **8605**, 86050U (2013).
2) H. Nasim and Y. Jamil, Opt. Laser Technol. **56**, 211 (2014).
3) Y. Liu, G. Yang, Z. Wang, T. Li, S. Tang, Y. Zhao, Y. Lan, and A. Demir, Opt. Laser Technol. **141**, 107145 (2021).
4) Z. Sun, R. Li, Y. Bi, C. Hu, Y. Kong, G. Wang, H. Zhang, and Z. Xu, Opt. Laser Technol. **37**, 163 (2005).
5) H. Wang, W. Huang, Z. Zhou, and H. Cao, Opt. Laser Technol. **36**, 69 (2004).
6) L. F. Johnson, J. E. Geusic, and L. G. Van Uitert, Appl. Phys. Lett. **7**, 127 (1965).
7) K. Fujioka, T. Murakami, S. Motokoshi, T. Yanagitani, H. Yoshida, K. Tsubakimoto, K. Yamamoto, and N. Miyanaga, Opt. Mater. **128**, 112396 (2022).
8) S. Radmard, A. Haghparast, S. Arabgarin, and M. T. Mehrabani, Opt. Laser Technol. **48**, 44 (2013).
9) M. Javadi-Dashcasan, F. Hajiesmaeilbaigi, H. Razzaghi, M. Mahdizadeh, and M. Moghadam, Opt. Commun. **281**, 4753 (2008).
10) B. Dannecker, J. Negel, A. Loescher, P. Oldorf, S. Reichel, R. Peters, T. Graf, and M. A. Ahmed, Opt. Commun. **429**, 180 (2018).
11) C. H. Kim and D. C. Ahn, Opt. Laser Technol. **44**, 1874 (2012).
12) C. Leone, S. Genna, F. Tagliaferri, B. Palumbo, and M. Dix, Opt. Laser Technol. **76**, 127 (2016).
13) M. R. Kumar, I. Tomashchuk, J. M. Jouvard, and M. Duband, J. Advanced Joining Processes **5**, 100097 (2022).
14) F. Zhuang, Q. Shu, D. Gong, and G. Zhang, Opt. Mater. **107**, 110146 (2020).
15) H. Hugel and W. L. Bohn, Proc. of SPIE **3574**, 16 (2022).
16) S. Nakamura, H. Yoshioka, Y. Matsubara, T. Ogawa, and S. Wada, Opt. Commun. **281**, 4411 (2008).
17) G. Ma et al., Opt. Laser Technol. **92**, 32 (2017).
18) F. Zhuang, Qe Shu, D. Gong, and G. Zhang, Opt. Mater. **107**, 110146 (2020).
19) C. Schnitzler, S. Hambuecker, O. Ruebenach, V. Sinhoff, G. Steckman, L. West, C. Wessling, and D. Hoffmann, Proc. of SPIE **6456**, 645612 (2007).
20) B. Köhler, T. Brand, M. Haag, and J. Biesenbach, "Wavelength stabilized high-power diode laser modules," Proc. of SPIE **7198**, 719810 (2009).
21) J. Han, J. Zhang, X. Shan, Y. Zhang, H. Peng, L. Qin, and L. Wang, Optik **264**, 169455 (2022).
22) Z. Yang, H. Wang, Y. Li, Q. Lu, W. Hua, X. Xu, and J. Chen, Opt. Commun. **284**, 5189 (2011).
23) J. Pierer, M. Lützelschwab, S. Grossmann, G. S. Durante, C. Bosshard, B. Valk, R. Brunner, R. Bättig, and N. Lichtenstein, Proc. of SPIE **7918**, 791801 (2011).
24) R. Liu et al., Proc. of SPIE **9348**, 93480V (2015).
25) Y. Li, V. Negoita, T. Barnowski, S. Strohmaier, and G. Treusch, IEEE Photonics Society Summer Topical Meeting Series , 2012, p. 29.
26) B. Leonhäuser, H. Kissel, J. W. Tomm, M. Hempel, A. Unger, and J. Biesenbach, Proc. of SPIE **9348**, 93480M (2015).

